Sn(IV) Sorption Onto Illite and Boom Clay: Effect of Carbonate and Dissolved Organic Matter

Delphine Durce [1,*], Sonia Salah [1], Liesbeth Van Laer [1], Lian Wang [1], Norbert Maes [1], Stéphane Brassinnes [2]

[1] Belgian Nuclear Research Centre (SCK-CEN), Expert Group Waste & Disposal, Boeretang, 2400 Mol, Belgium

[2] ONDRAF-NIRAS, Belgian Agency for Radioactive Waste and Enriched Fissile Materials, Avenue des Arts 14, 1210 Bruxelles, Belgium

* Correspondence: delphine.durce@sckcen.be; Tel.: +32-14-33-32-32

Table S1. Cationic composition of the clay suspensions. n.m = not measured. D.L = detection limit. The measurement errors were not provided but they were estimated to $2\sigma[conc/[conc] = 0.1.$ for all the elements, but for Sn in IdP_0, which was estimated to $2\sigma[conc/[conc] = 0.2$ (close to detection limit).

Concentrations in mol/L	IdP_0	IdP_1	BC_1
Na	n.m	n.m	n.m
Mg	3.15 E-05	1.85E-05	1.26E-05
Al (NoGas)	2.81E-05	3.44E-05	3.90E-06
Al (He)	2.86E-05	3.55E-05	4.34E-06
Si	3.48E-04	8.90E-04	6.84E-04
P	1.12E-01	8.30E-02	2.40E-05
K	6.29E-05	1.54E-04	2.88E-04
Ca	3.76E-05	2.53E-05	2.94E-04
Ti	3.12E-07	1.56E-07	1.33E-06
Fe	1.13E-06	6.96E-07	7.54E-06
Cu	8.67E-06	1.55E-07	4.16E-07
Zn	4.94E-05	4.30E-07	1.33E-06
Sn	6.01E-09	< D.L	2.05E-08

Table S2. Composition of the SPRING water measured by ICP-MS and Ionic Chromatography.

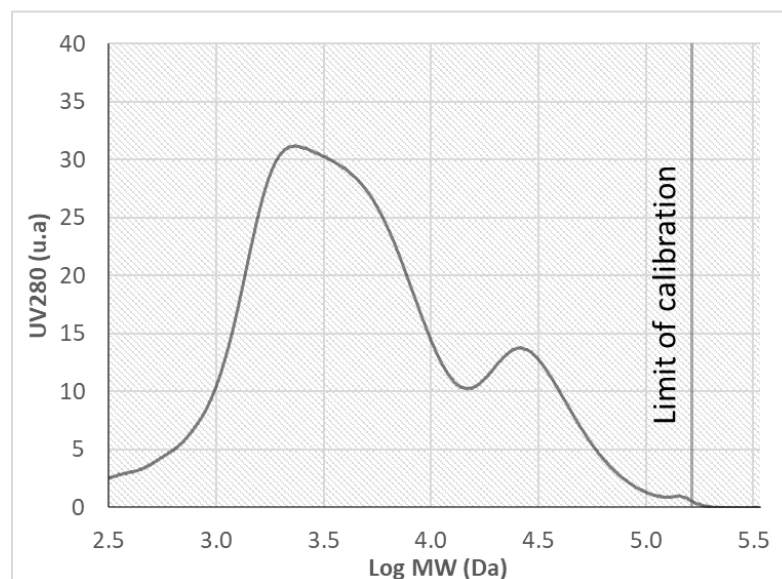| Elements	Concentrations in mg/L
B	7.79 ± 0.18
Ca	2.64 ± 0.1
Fe	0.53 ± 0.14
K	10.0 ± 0.8
Mg	2.22 ± 0.14
Na	358 ± 29
Si	4.12 ± 0.12
Sr	0.071 ± 0.036
F	3.3 ± 0.5
Cl	19.5± 0.8
Br	0.72 ± 0.20
SO_4	< 0.8
S_2O_3	< 2

Figure S1. Molecular Weight (MW) Distribution of DOM_NaClO$_4$ measured by SEC/UV280.
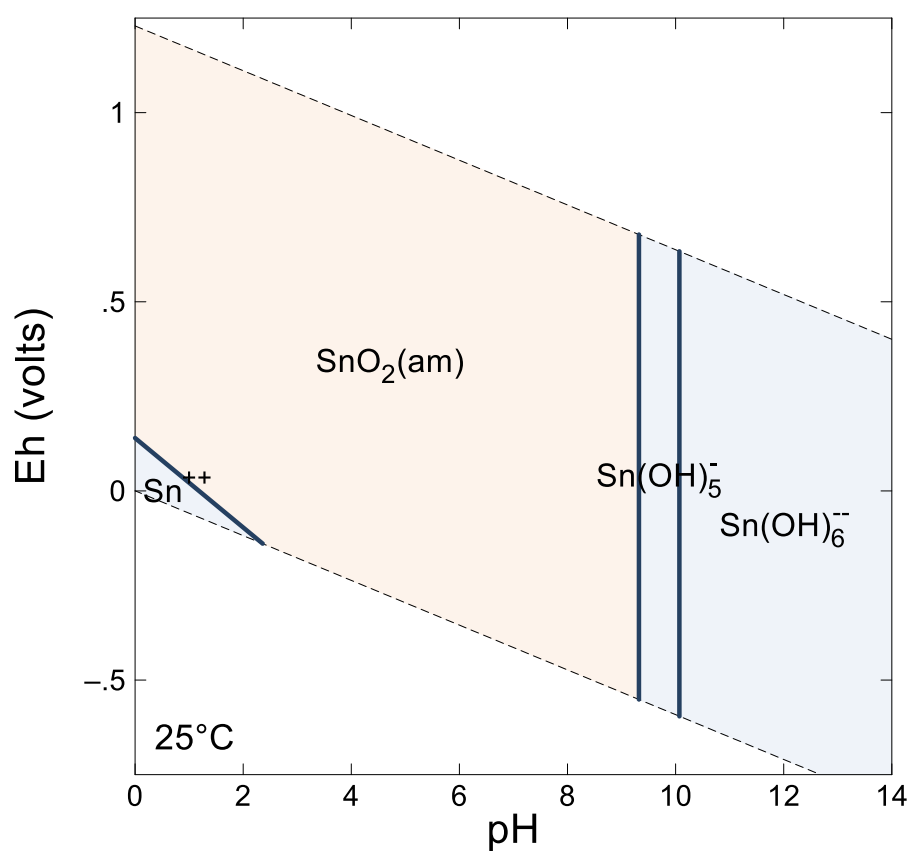

Figure S2. Eh-pH diagram for Sn. database: ThermoChimie 10d, computer code GWB 16. Sn activity 3.1 ×10^{-7}, NaClO$_4$ activity 0.017. Casserite was not allowed to precipitate.
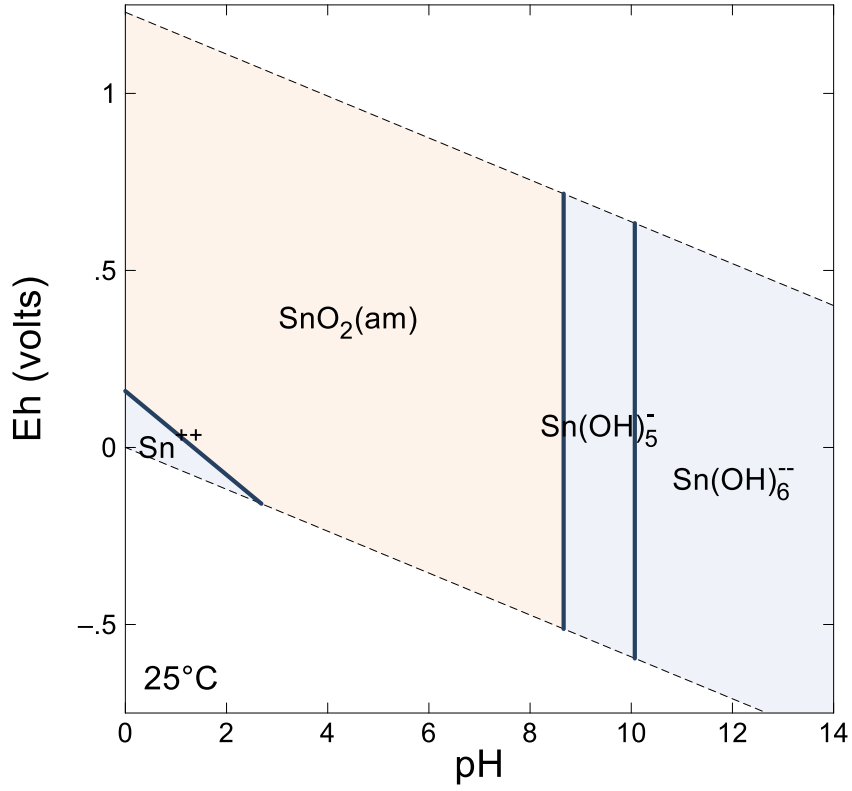
Figure S3. Eh-pH diagram for Sn. database: ThermoChimie 10d, computer code GWB 16. Sn activity 6.8 ×10⁻⁸, NaClO₄ activity 0.017. Casserite was not allowed to precipitate.

Uncertainty calculation for distribution coefficients R_d

The interaction constant is calculated as:

$$R_d = \frac{Sn_0 - Sn_{eq}}{Sn_{eq}} \times \frac{V}{m}$$

(S1)

With Sn_0 and Sn_{eq} calculated as

$$Sn_{0/eq} = \frac{(CPM_s - CPM_b)}{V_s \times 60 \times \varepsilon \times e^{\left(\frac{ln2}{t_{1/2}} \times \Delta t\right)}} \times \frac{C_0}{A_0}$$

(S2)

And

$$SCPM_0 \; or \; SCPM_{eq}\left(\frac{CPM}{mL}\right) = \frac{CPM_s - CPM_b}{V_s}$$

(S3)

Combination of (1), (2) and (3) gives:

$$R_d = \frac{SCPM_0 - SCPM_{eq}}{SCPM_{eq}} \times \frac{V}{m}$$

(S4)

The uncertainty of R_d is calculated by propagating the experimental errors (confidence limit of 95 %), according to equation:

$$2\sigma(R_d) = R_d * \sqrt{\frac{2\sigma(SCPM_0)^2 + \sigma\left(SCPM_{eq}\right)^2}{\left(SCPM_0 - SCPM_{eq}\right)^2} + \frac{2\sigma\left(SCPM_{eq}\right)^2}{\left(SCPM_{eq}\right)^2} + \frac{2\sigma(V)^2}{(V)^2} + \frac{2\sigma(m)^2}{(m)^2}}$$

(S5)

And

$$2\sigma\left(SCPM_0 \text{ or } SCPM_{eq}\right) = \left(SCPM_0 \text{ or } SCPM_{eq}\right) * \sqrt{\frac{2\sigma(CPM_s)^2 + 2\sigma(CPM_b)^2}{(CPM_s - CPM_{bck})^2} + \frac{2\sigma(V_s)^2}{(V_s)^2}} \quad \text{(S6)}$$

where $SCPM_0$ and $SCPM_{eq}$ are the specific counts of the suspensions and the supernatants, CPM_s and CPM_b are the measured counts in LSC of the sample and the background, respectively, V and V_s, the total solution volume of the sorption experiments and the sample volume measured in LSC, respectively, and m, the mass of clay in the sorption experiments. The value $2\sigma(V)/V=0.05$, $2\sigma(m)/m=0.05$ and the error of the sampled volume were assumed negligible, i.e $2\sigma(V_s)/V_s=0.0$

Sensitivity analysis for the determined complexation constants

The sensitivity of all the determined constants to the most influent input parameters was estimated. With respect to the Sn(IV) hydrolysis constants, only the influence of $log\ K^4_{OH}$ and $log\ K^5_{OH}$ values was evaluated. $Sn(OH)_6^{2-}$ is not sorbing and its contribution to the model was, therefore, neglected. With respect to the IdP protolysis constants, only the influence of the deprotonation constant of the strong sorption site, referred to as $log\ KS^s_{O-,}$ was evaluated. The protonation of the strong sites occurs at low pH and its contribution to the sorption of Sn(IV) in our experimental conditions (pH ~8.4) was assumed negligible.

The sensitivity of the fitted complexation constants ($log\ K_3$ to $log\ K_{7/8}$) and of the strong sorption site capacity ($\equiv \boldsymbol{S^sOH}$) to the selected input parameters was evaluated within the boundaries of the confidence intervals of the latter. The input parameters were varied independently to the highest and lowest boundary of their confidence intervals and the complexation constants were fitted for each condition, as reported in the 'modelling' section of the paper.

The resulting variation in the values of the fitted complexation constants are reported in Figures ES4 to ES9. It can be seen that the sensitivity of the fitted complexation constants to the input parameters was variable and, while some constants were the most sensitive to the formation of $Sn(OH)_4$, others were strongly dependent on the deprotonation of the sorption site. However, the sensitivity to the formation of $Sn(OH)_5^-$ remained, overall, smaller in our experimental conditions.
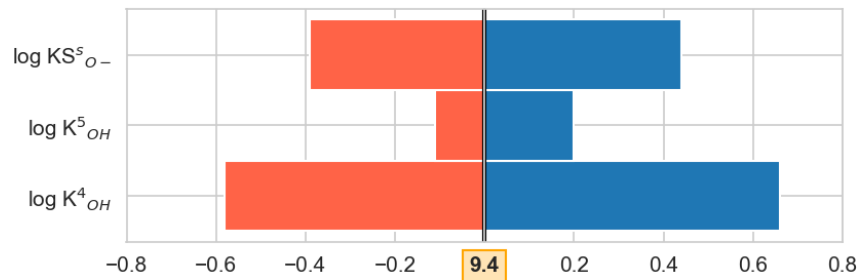

Figure S4. Variation of $log\ K_3$ around its optimized value with the variation of the input parameters $log\ K^4_{OH}$, $log\ K^5_{OH}$ and $log\ KS^s_{O-}$. In orange: variation induced by using the lowest boundary of the input parameters confidence interval. In blue: variation induced by using the highest boundary of the input parameters confidence interval.
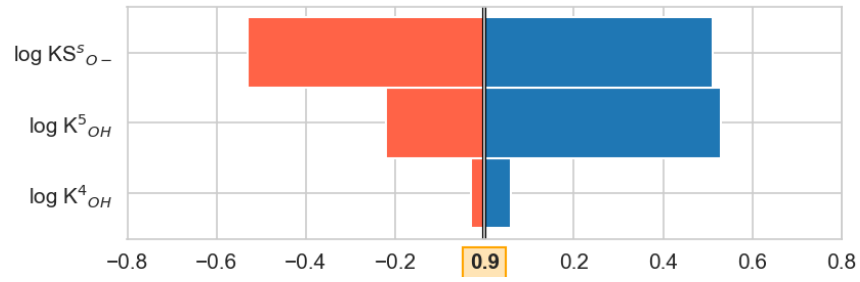
Figure S5. Variation of *log K_4* around its optimized value with the variation of the input parameters *log K^4_{OH}, log K^5_{OH} and log KS^s_{O-}*. In orange: variation induced by using the lowest boundary of the input parameters confidence interval. In blue: variation induced by using the highest boundary of the input parameters confidence interval.
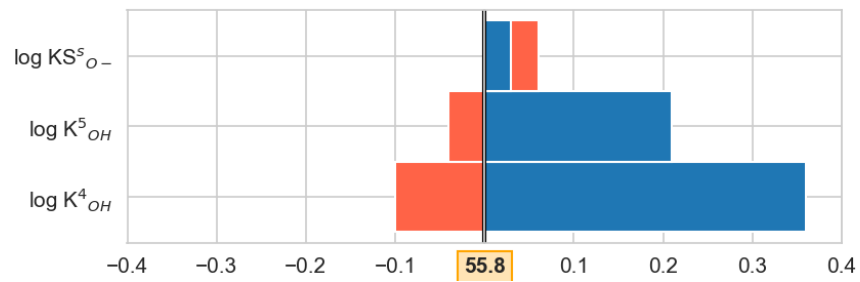

Figure S6. Variation of *log K_5* around its optimized value with the variation of the input parameters *log K^4_{OH}, log K^5_{OH} and log KS^s_{O-}*. In orange: variation induced by using the lowest boundary of the input parameters confidence interval. In blue: variation induced by using the highest boundary of the input parameters confidence interval.
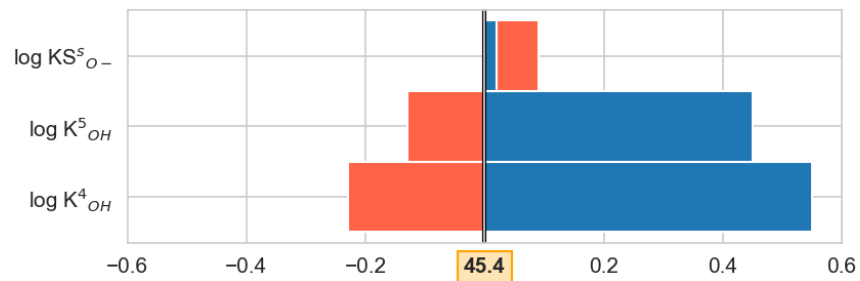

Figure S7. Variation of *log K_6* around its optimized value with the variation of the input parameters *log K^4_{OH}, log K^5_{OH} and log KS^s_{O-}*. In orange: variation induced by using the lowest boundary of the input parameters confidence interval. In blue: variation induced by using the highest boundary of the input parameters confidence interval.
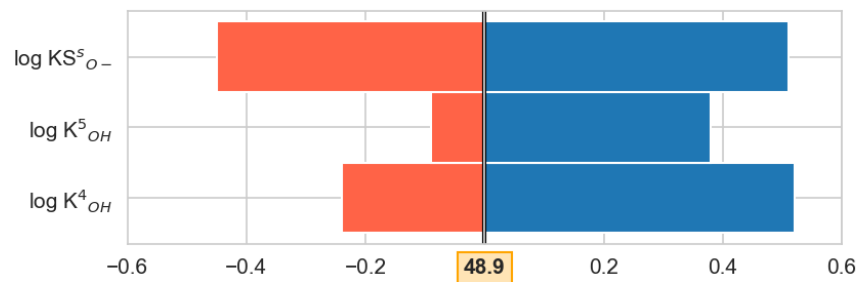

Figure S8. Variation of *log $K_{7/8}$* around its optimized value with the variation of the input parameters *log K^4_{OH}, log K^5_{OH} and log KS^s_{O-}*. In orange: variation induced by using the lowest boundary of the input parameters confidence interval. In blue: variation induced by using the highest boundary of the input parameters confidence interval.
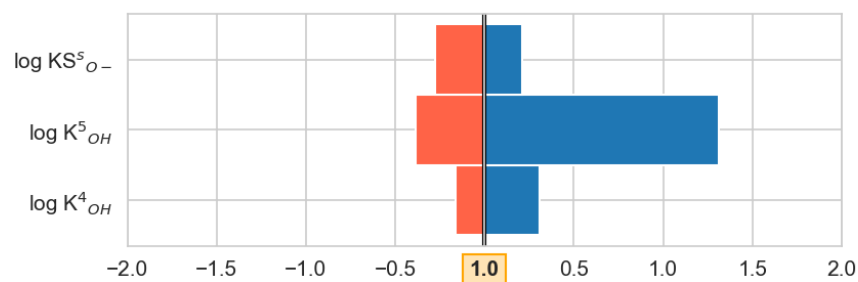
Figure S9. Variation of $\equiv S^sOH$ ($\times 10^{-3}$ mol/L) around its optimized value ($\times 10^{-3}$ mol/L) with the variation of the input parameters log K^4_{OH}, *log K^5_{OH} and log $KS^s_{O^-}$*. In orange: variation induced by using the lowest boundary of the input parameters confidence interval. In blue: variation induced by using the highest boundary of the input parameters confidence interval.